

1190

~~6410~~

~~562~~

~~52~~

*Library, L. M. A. L.*

TECHNICAL MEMORANDUMS

NATIONAL ADVISORY COMMITTEE FOR AERONAUTICS

No. 763

THE HEAT TRANSFER OF COOLING FINS ON MOVING AIR

By Hans Doetsch

Abhandlungen aus dem Aerodynamischen Institut  
an der Technischen Hochschule Aachen  
No. 14, 1934

**FILE COPY**  
To be returned to  
the files of the Langley  
Memorial Aeronautical  
Laboratory.

Washington  
January 1935

RECEIVED JAN 15 1935



3 1176 01441 1509

NATIONAL ADVISORY COMMITTEE FOR AERONAUTICS

TECHNICAL MEMORANDUM NO. 763

THE HEAT TRANSFER OF COOLING FINS ON MOVING AIR\*

By Hans Doetsch

SUMMARY

The present report is a comparison of the experimentally defined temperature and heat output of cooling fins in the air stream with the theory. The agreement is close on the basis of a mean coefficient of heat transfer with respect to the total surface. A relationship is established between the mean coefficient of heat transfer, the dimensions of the fin arrangement, and the air velocity.

I. INTRODUCTION

The use of cooling fins is advisable in cases where with thermal conduction through metallic walls, the coefficients of heat transfer on the two sides are widely at variance. The thermal conductivity is, as known, lower than the minimum coefficient of heat transfer. Now, the passage of heat may be improved by providing cooling fins at the side of the lower thermal conductivity, which increases the heat exchanging surface. But owing to its lower temperature, the fin surface is not as efficient as the base surface to which the fins are attached.

Let:  $y$  = distance from root of fin (m),

$h$  = fin depth (m),

$\vartheta$  = temperature difference between fin and cooling medium at point  $y$  ( $^{\circ}\text{C}$ ),

$\vartheta_0$  = temperature difference between base surface and cooling medium ( $^{\circ}\text{C}$ ),

$\alpha$  = coefficient of heat transfer  $\left(\frac{k \text{ cal}}{\text{m}^2 \text{ h } ^{\circ}\text{C}}\right)$

---

\*"Die Wärmeübertragung von Kühlrippen an strömende Luft."  
Abhandlungen aus dem Aerodynamischen Institut an der  
Technischen Hochschule Aachen, No. 14, 1934, pp. 3-23.

The amount of heat given off per meter of fin side is:

$$Q = \alpha \int_0^h \vartheta dy \left[ \frac{\text{k cal}}{\text{m h}} \right]$$

If the temperature of the fin side were that of base surface  $\vartheta_0$  the amount of heat removed would be:

$$Q_0 = \alpha \vartheta_0 h \left[ \frac{\text{k cal}}{\text{m h}} \right]$$

Thus the efficiency of the fin surface can be expressed with:

$$\eta_R = \frac{\alpha \int_0^h \vartheta dy}{\alpha \vartheta_0 h} = \frac{\int_0^h \vartheta dy}{\vartheta_0 h}$$

In order to determine the heat removal from the fin, we must first define the temperature in the fin. This problem may be treated by means of the differential equations of heat conduction.

For the practice, however, the following question needs to be elucidated: In the case of closely spaced fins, the coefficient of heat transfer  $\alpha$  varies for a stated flow attitude of the cooling medium considerably from coefficient of heat transfer of the flat wall. The evaluation of the effectiveness of a fin arrangement and the analysis of the transferred heat volume is contingent upon the relationship existing between coefficient of heat transfer and flow velocity and the dimensions of the fin arrangement. This problem cannot be solved theoretically. The magnitude of the coefficient of heat transfer must be determined from experiments.

The purpose of the present report is first to compare the temperature distribution and heat output of the fin as obtained from the differential equation of heat conduction with the experimentally defined values, and then to determine the magnitude of the coefficient of heat transfer for a number of fin arrangements and velocities. An attempt was to be made to establish a relationship for the coefficient of heat transfer with respect to the velocity and the dimensions of the fin arrangement.

The investigations were made on plates with straight cooling fins into air. This case is mathematically and experimentally more readily tractable than the technically equally important case of circumferential fin on a finned tube. Obviously certain results and inferences are equally applicable to round fins.

## II. THEORETICAL PRINCIPLES

The simplifying assumptions preceding the calculation of the cooling fins are:

1. The amount of heat given off into the air by the fin surface in unit time is proportional to the temperature difference between surface and undisturbed air stream;
2. The coefficient of heat transfer is constant over the whole fin surface;
3. The temperatures are steady;
4. The temperature at the fin root is constant;
5. The temperature over the fin thickness is constant;
6. The effect of the fin ends is disregarded.

### Notation

- $\alpha$ , coefficient of heat transfer  $[\frac{k \text{ cal}}{m^2 h ^\circ C}]$
- $\lambda$ , thermal conductivity of the fin material  $[\frac{k \text{ cal}}{m h ^\circ C}]$
- $\vartheta$ , temperature difference between fin and undisturbed stream ( $^\circ C$ )
- $z_0$ , semifin thickness at root (m)
- $h$ , fin depth (m)
- $y$ , distance from root of fin (m)

The differential equation for the straight rectangular fin (fig. 1a) is:

$$\frac{d}{dy} \left( \lambda z_0 \frac{d\vartheta}{dy} \right) = \alpha \vartheta$$

$$\frac{d^2\vartheta}{dy^2} - \frac{\alpha}{\lambda z_0} \vartheta = 0$$

The general solution for  $\vartheta$  is:

$$\vartheta = A e^{\sqrt{\frac{\alpha}{\lambda z_0}} y} + B e^{-\sqrt{\frac{\alpha}{\lambda z_0}} y}$$

The heat carried off at the fin head is disregarded for the present. Then the boundary conditions are:

$$\vartheta = \vartheta_0 \quad \text{for } y = 0;$$

$$\frac{d\vartheta}{dy} = 0 \quad \text{for } y = h.$$

With  $m = \sqrt{\frac{\alpha}{\lambda z_0}}$ , it gives:

$$A = \vartheta_0 \frac{e^{-mh}}{e^{mh} + e^{-mh}}; \quad B = \vartheta_0 \frac{e^{mh}}{e^{mh} + e^{-mh}}$$

$$\vartheta = \vartheta_0 \frac{\cosh m(y - h)}{\cosh mh}$$

The temperature at the fin tip for  $y = h$  is:

$$\vartheta_{RS} = \frac{\vartheta_0}{\cosh \sqrt{\frac{\alpha}{\lambda z_0}} h}$$

The heat removal per meter of fin side is:

$$Q = \alpha \int_0^h \vartheta dy$$

The insertion of the term for  $\vartheta$  followed by integration gives:

$$\frac{Q}{y_0} = \sqrt{\alpha \lambda z_0} \tanh \sqrt{\frac{\alpha}{\lambda z_0}} h \left[ \frac{k \text{ cal}}{m \cdot h \cdot ^\circ C} \right]$$

The amount of heat leaving the head of the fin can be approximately allowed for in the heat-output equation when using quantity  $(h + z_0)$  instead of  $h$  for fin depth.

The differential equation for the straight triangular fin (fig. 1b) is:

$$\frac{d}{dy} \left( \lambda z \frac{d\vartheta}{dy} \right) = \alpha \vartheta.$$

In this case the fin thickness is a function of  $y$ . With

$$z = \frac{z_0}{h} y$$

we have:

$$\frac{d^2 \vartheta}{dy^2} + \frac{1}{y} \frac{d\vartheta}{dy} - \frac{\alpha h}{\lambda z_0} \frac{\vartheta}{y} = 0$$

The equation is simplified by substituting

$$v = \frac{\alpha h}{\lambda z_0} y$$

so that:

$$\frac{d^2 \vartheta}{dv^2} + \frac{1}{v} \frac{d\vartheta}{dv} - \frac{\vartheta}{v} = 0$$

The general solution reads:

$$\vartheta = A J_0 (2i \sqrt{v}) + B N_0 (2i \sqrt{v})$$

$J_0$  and  $N_0$  are Bessel functions of zero order with imaginary arguments.

As  $\vartheta$  must be positive real for  $y = 0$ , the solution reduces to

$$\vartheta = A J_0 (2i \sqrt{v})$$

With the boundary condition:  $\vartheta = \vartheta_0$  for  $y = h$  and reinsertion of the term for  $v$ , it is:

$$\vartheta = \vartheta_0 \frac{J_0 \left( 2i \sqrt{\frac{\alpha}{\lambda z_0}} \sqrt{y h} \right)}{J_0 \left( 2i \sqrt{\frac{\alpha}{\lambda z_0}} h \right)}$$

The temperature at the fin tip is for  $y = 0$ :

$$\vartheta_{RS} = \frac{\vartheta_0}{J_0 \left( 2i \sqrt{\frac{\alpha}{\lambda z_0}} h \right)}$$

The heat dissipation per meter of fin side is:

$$Q = \alpha \int_0^h \vartheta dy$$

The term for  $\vartheta$  is introduced and integration gives:

$$\frac{Q}{\vartheta_0} = \sqrt{\alpha \lambda z_0} \frac{\left[ -i J_1 \left( 2i \sqrt{\frac{\alpha}{\lambda z_0}} h \right) \right]}{J_0 \left( 2i \sqrt{\frac{\alpha}{\lambda z_0}} h \right)} \left[ \frac{k \text{ cal}}{m h ^\circ C} \right]$$

For purposes of comprehensive graphical representation of temperature and heat dissipation of both fin forms a new nondimensional quantity is introduced and we write:

$$u = 4F \sqrt{\frac{\alpha}{\lambda}} z_0^{-3/2}$$

wherein  $F = \frac{z_0 h}{2}$ .

On the rectangular fin  $F = \frac{1}{4}$  of the fin section; on the triangular fin  $F = \frac{1}{2}$  fin section. The heat output of the rectangular fin is:

$$\frac{Q}{\vartheta_0} = \sqrt{\alpha \lambda} \sqrt[3]{4F \sqrt{\frac{\alpha}{\lambda}}} u^{-1/3} \tanh \frac{u}{2}$$

The temperature at the fin tip is:

$$\vartheta_{RS} = \frac{\vartheta_0}{\cosh \frac{u}{2}}$$

The equivalent terms for the triangular fin are:

$$\frac{Q}{\vartheta_0} = \sqrt{\alpha \lambda} \sqrt[3]{4F \sqrt{\frac{\alpha}{\lambda}}} u^{-1/3} \frac{[-i J_1(iu)]}{J_0(iu)}$$

and

$$\vartheta_{RS} = \frac{\vartheta_0}{J_0(iu)}$$

The equations of heat dissipation for the rectangular and triangular fin are identical in construction, except for the Bessel instead of the hyperbolical functions on the triangular fin.

Figure 2 shows the dimensionless term  $\frac{Q}{\vartheta_0 \sqrt{\alpha \lambda} \sqrt[3]{4F \sqrt{\frac{\alpha}{\lambda}}}}$

against  $u$  for both fin forms. Both functions manifest a maximum. This means that with fixed  $\alpha$ ,  $\lambda$ , and  $F$  values, the heat output of the fin yields a maximum for a certain ratio of fin thickness to fin depth. In this case the material required for a given heat output is minimum.

Figure 2 also manifests that the heat output of the rectangular fin is not substantially higher than that of the triangular fin of identical thickness at the base and identical height. The margin of the first over the latter is greatest near the maximum of the two functions, i.e., about 11.5 percent in this particular case.

This small gain in output is faced with twice as great an amount of material required. The triangular is preferable to the rectangular fin, for reasons of saving of material.

In figure 3 the fin-tip temperature for both types of fins is plotted against  $u$ . Here the discrepancies are more pronounced than with the heat output.

The exact triangular shape is not realizable in practice. The fins usually have a definite thickness at the tip; that is, they have a tapered section.

We reproduce the equations for wedge-shaped fins (fig. 1c) from Harper and Brown's report (reference 1):

$$\eta = \eta_0 \frac{H_1(ib_0) J_0(ib_y) + i H_0(ib_y) i J_1(ib_0)}{H_1(ib_0) J_0(ib_h) + i H_0(ib_h) i J_1(ib_0)}$$

$$\frac{Q}{\eta_0} = \frac{\alpha b_h}{2g^2 \cos \delta} \frac{H_1(ib_h) i J_1(ib_0) - i J_1(ib_h) H_1(ib_0)}{H_1(ib_0) J_0(ib_h) + i J_1(ib_h) i H_0(ib_h)} \left[ \frac{k \text{ cal}}{m h \text{ } ^\circ\text{C}} \right]$$

wherein

$$g = \sqrt{\frac{\alpha}{\lambda \sin \delta}}$$

$$b_0 = 2g \sqrt{\frac{z_h (1 - \tan \delta)}{\tan \delta}}$$

$$b_y = 2g \sqrt{y + \frac{z_h (1 - \tan \delta)}{\tan \delta}}$$

$$b_h = 2g \sqrt{h' + \frac{z_h (1 - \tan \delta)}{\tan \delta}}$$

Harper and Brown make an approximate allowance for the amount of heat flowing from the fin head by writing  $(h + z_h) = h'$  instead of height  $h$ .

The figures for the heat dissipation of the wedge-shaped fin range between those of the triangular and the rectangular fin, which form the boundary conditions for  $z_h = 0$  and  $z_h = z_0$ .

The numerical evaluation of Harper and Brown's equations is very tedious because of the complicated expression of the Bessel functions. In most cases the equations for the triangular fin will be serviceable as practical approximation, especially in cases where the thickness ratio of fin tip to fin root is small.

We shall forego all further theoretical considerations and refer, for the rest, to Harper and Brown's report (reference 1) and to E. Schmidt's report in the V.D.I. (reference 2).

## III. TEST ARRANGEMENTS AND PROCEDURE

The tests were made in the small wind tunnel of the Aachen Institute. The tunnel has an open experimental chamber and an entrance cone of 500 by 300 mm (19.69 by 11.82 in.). The air is supplied by a fan in a closed circuit. The hollow guide vanes of the tunnel can be connected to the water system and serve to cool the air stream. The rough control of the air velocity was obtained by adjusting the terminal voltage of the engine; the fine control, by regulating the field current.

The program included a flat plate without fins and six fin specimens. The plates were exposed to the air stream parallel to the base and parallel to the fins. The length in the flow direction was 500 mm in all cases, the width of the plates 210 mm (8.27 in.). The changes effected on the finned plates included depth, spacing, and thickness at fin root. The dimensions of the examined plates are appended in table I. The flat plate and finned plate No. 1 were of ultralumin, the others of silumin. The thermal conductivity of the material was obtained from coupons by the Phys.-Techn. State Institute at Berlin.. It amounted to:

$$\lambda = 145 \left[ \frac{\text{k cal}}{\text{m h } ^\circ\text{C}} \right] \text{ for ultralumin}$$

and

$$\lambda = 142 \left[ \frac{\text{k cal}}{\text{m h } ^\circ\text{C}} \right] \text{ for silumin}$$

The finned plates were machined from a solid casting, thus assuring an accurate fin profile and a smooth surface.

The test plate was built up with a detachable frame and a top of identical material into a flat box, screwed together by means of cap screws on the rear side, so as to insure a smooth front surface devoid of holes or screw heads.

The thus built-up box was filled with oil and contained in addition a heating resistance consisting of individually controllable constantan wire coils. The heating elements were mounted perpendicular to the direction of air flow, and the switching on and off of individual elements assured a constant plate temperature in the flow direction as desirable for the purpose of comparing the results with the theory. Two agitators (stirrers) in the

box, activated from the back of the box, provided an appropriate swirl of the oil.

The four narrow sides of the box were sheeted in a wooden frame, its front forming a pointed entering edge. On the finned plates the metal fins extended over the width of this flow profile with equally tapered wooden fin. This arrangement served to effect an undisturbed entry of the air into the passage between every two fins and to provide a uniform formation of the velocity boundary layers of the fin sides and the base surface. The narrow back of the box was fitted with a longer, parallel piece of wood, thus assuring a more equal velocity distribution over the tunnel section. In order to minimize the heat loss of the experimental set-up, the lid of the box - that is, the surface facing the experimental plate - was outwardly covered by an "expansit" plate of 5 cm (1.97 in.) thickness. Figure 4 is a sketch of the experimental box with covering. For better guidance of the air the plate was covered on top and bottom by boards spaced to correspond to the 300 mm height of the entrance cone.

Below the test plate was a lathe bed set on concrete, on which the speed and temperature recording instruments could be mounted.

The measurements in the principal tests were those of air velocity, electric power input, temperature of base plate, fins, lid, and air temperature.

Velocity.- The air velocity was measured with a Prandtl pitot tube and a Prandtl dynamic pressure indicator. The necessary constant velocity of the undisturbed flow along the plate was maintained by different devices. The velocity field between the fins was measured with a fine pitot tube of 0.25 mm (0.01 in.) inside and 0.4 mm (0.016 in.) outside diameter. It was made from a bent hypodermic needle soldered onto a larger tube. The orifice of the needle was carefully polished. Comparison with a standard pitot tube revealed perfect agreement after an adjustment interval of about 2 minutes.

Power.- The electric heat input was determined with a Siemens precision ammeter and voltmeter.

Temperature.- It was measured with constantan and manganin thermocouples, soldered together prior to mounting on the plate and artificially aged about 24 hours through

an electrical current. Subsequently they were calibrated in a thermostat filled with transformer oil by comparison with a mercury thermometer tested in the Phys. Techn. Institute. The hot junction of the element was pressed against the thermometer bulb and dipped directly in the oil, while the cold junction was in a thermostat filled with crushed ice during the calibration and the test. The surface thermocouples were soldered in grooves with duralumin solder.

To check the absence of changes in thermal force due to the heating of the junction during soldering to the plate, several thermocouples were carefully cut out along with a small strip of the plate and tested again in the thermostat. A comparison with the previously obtained test curve revealed an exact accord.

Owing to the numerous temperature stations the compensation method was too tedious, thus the thermal current was measured with a Siemens-Halske needle galvanometer and moving coil measuring instrument and strip suspension. The deflection was adapted to the temperature differences by means of suitable series resistances. The elements pertaining to a cold junction were all of the same length and within one common calibration curve. The ratio of galvanometer deflection to temperature difference was plotted against galvanometer deflection which made for more convenient evaluation. The test curves within the explored temperature range were straight. The base-plate temperature was determined with 12 thermocouples of 0.5 mm (0.02 in.) diameter soldered on the inside of the base plate. This made it necessary to compute the temperature of the surface exposed to the air by ascertaining the temperature gradient in the wall, but it precluded a disturbance of the velocity field before the plate otherwise occurring if the thermocouples had been mounted on the outside.

The temperature gradient in the wall follows from

$$Q_p = \frac{\lambda F_0 \Delta t}{s}$$

where  $Q_p$  = heat dissipation of plate per hour into air,

$\lambda$  = thermal conductivity of the material,

$F_0$  = base surface of plate,

$s$  = plate thickness.

The temperature gradient in the wall during the tests ranged between 0.2 and 1.5 percent of the gradient between base and air, depending on the heat charge of the plate.

Starting from the junctions, the thermocouple wires passed in sets of 4's through carefully sealed openings to the wooden frame and from there to the switch panel.

The temperature of the side of a fin was measured at different points from the plate edge with 0.3 mm (0.012 in.) thermocouples, which afforded the fin temperature in/and perpendicular to the flow direction. The temperature in the undisturbed air stream was obtained with a fixed thermocouple on the entrance cone and a second one adjustable in/and perpendicular to the direction of flow. It was constant in all tests within range of the test plate. The temperature of the lid on the back and the temperature on the surface of the wooden frame were also recorded.

Boundary layer thermocouple.- The temperature in the boundary layer between the fins was recorded with a special thermocouple for point-temperature reading (fig. 5). The glass tube is of 0.5 mm (0.02 in.) outside and 0.3 mm (0.012 in.) inside diameter, open on both ends, the junction of the 0.05 mm (0.002 in.) thermocouple wires lying directly at the front opening. The wires pass along the outside of the tube to the glass holder.

This thermocouple was checked in boundary-layer tests of a flat plate and compared with another thermocouple of known arrangement as used by F. Eliás (reference 3). The test data were in perfect accord for this two-dimensional case, so that a temperature record sufficiently accurate for our purposes was likewise expected for the three-dimensional case of boundary layer between fins.

Loss experiments.- The heat given off by the test plate into the air constituted the difference between the electrical heat input and the heat losses of the test set-up. The heat losses occurred chiefly on the exposed back of the test arrangement and on the front of the frame. The losses on the back and on the upper and lower parts of the frame not exposed to the air, were determined separately.

To this end the test box was fitted with a flat plate and carefully insulated at both front and back so as to

assure symmetry in the new arrangement about the median plane of the oil-filled box.

The power input of this arrangement was determined for different air velocities concurrently with the temperature at the front and back of the test box. The mean temperatures on the front and back were the same during all loss experiments. In a test with the normal experimental set-up the heat loss on the back and narrow sides of the wooden frame for equal temperature over the air of the box lid and for equal air velocities had to be equal to half the power absorbed with the new arrangement. The loss at the front of the wooden frame was determined as follows: The temperature distribution on the surface of the wooden frame was recorded with eight thermocouples, and the mean temperature over the air  $\vartheta_{Ra}$  of the frame was plotted, thus giving the frame losses with

$$Q_{Ra} = \vartheta_{Ra} F_{Ra} \alpha$$

where  $F_{Ra}$  = proportion of frame surface promoting heat dissipation,

$\alpha$  = heat transfer coefficient defined from tests on flat plates.

There were also radiation losses. The heat exchange through radiation between two surfaces  $F_0$  and  $F_1$  is

$$Q_{01} = F_0 C_{01} \left[ \left( \frac{T_0}{100} \right)^4 - \left( \frac{T_1}{100} \right)^4 \right] \left[ \frac{k \text{ cal}}{h} \right]$$

Here  $T_0$  = absolute temperature of plate surface ( $^{\circ}\text{C}$ ),

$T_1$  = " " " surrounding surfaces ( $^{\circ}\text{C}$ ),

$F_0$  = area of plate ( $\text{m}^2$ ),

$C_{01}$  = effective radiation  $\left[ \frac{k \text{ cal}}{\text{m}^2 (\text{^{\circ}\text{C}})^4 h} \right]$

The exact determination of  $C_{01}$  is limited to a few technical cases only.

For computing the radiation losses of the flat plate, we resorted to Nusselt's approximation formula for  $C_{01}$  (reference 4):

$$C_{o1} = C_o \frac{C_1}{C_s}; \quad C_o = \epsilon_o C_s; \quad C_1 = \epsilon_1 C_s$$

$C_s$  is the radiation constant of the absolutely black body.  
 $C_s = 4.96.$

For polished Al.  $\epsilon_o = 0.13$ ; for masonry  $\epsilon_1 = 0.93$

$$C_{o1} = \epsilon_o \epsilon_1 C_s = 0.6 \frac{\text{k cal}}{\text{m}^2 (\text{°C})^4 \text{ h}}$$

The radiation loss of the flat plate amounted to 0.6 to 1.5 percent of the heat energy.

As concerns the finned plates, the radiation is not easily computable because of the complicated mutual interference between the adjacent fins. The radiation heat of the finned plates relative to the heat by conduction could be neglected during the temperatures maintained in the tests. The total heat output loss in the flat-plate test averaged about 18 percent, and around 5 to 8 percent for the explored finned plates.

Principal tests.— These were chiefly made at night because of the voltage fluctuations in the power lines during daytime. The plate was first brought to the desired temperature with running stirrer and still air. Then the fan was started and the air velocity regulated. As a rule it was possible to reach the desired steady state after four to five hours by means of the water-cooling system of the wind tunnel. Heat output, air velocity, air temperature, and plate temperature were observed during the whole test, which was terminated only after the temperatures had remained stationary for two hours.

#### IV. RESULTS OF TESTS - EVALUATION

The investigation covered one flat plate and six finned plates at from 9 to 42 m/s (29.5 to 137.8 ft./sec.) air velocities. The temperature difference  $\vartheta_o$  between base plate and air was 36 to 40 °C in all tests. The evaluation was made on the basis of the figures corresponding to  $\frac{t_o + t_L}{2}$  temperature.

$t_o$  = temperature of plate surface  $F_o$ .

$t_L$  = temperature of undisturbed air stream.

The flat plate.— The results for the flat plate are given in figure 6, in comparison with the theory and Jürges' test data (table II) (reference 5).

For the turbulent range we computed von Kármán's and Latzko's data (reference 6) on the heat dissipation of a flat plate on the basis of the analogy between friction and heat transfer. This analogy is rigorously exact only when the Reynolds Number  $Re = UX/\nu$  equals the Peclet Number  $Pe = UXC/\lambda_L$ . Hereby,

$U$  = velocity of free air stream (m/s),

$X$  = plate length in stream direction (m),

$\nu$  = kinematic viscosity of the air ( $m^2/s$ ),

$C$  = specific heat of the air ( $k \text{ cal}/m^3 \text{ } ^\circ C$ ),

$\lambda_L$  = thermal conductivity of the air ( $k \text{ cal}/m \text{ h } ^\circ C$ ).

On these premises von Kármán and Latzko's calculations for the heat dissipation of a plate strip of width  $l$  up to point  $X$  gave:

$$Q(X) = 0.0356 C U \vartheta_o X \left(\frac{l}{RE}\right)^{1/5} \left[\frac{k \text{ cal}}{m \text{ s}}\right]$$

The conventional coefficient of heat transfer  $\alpha$  (expressed in  $k \text{ cal}/m^2 \text{ h } ^\circ C$ ) is:

$$\alpha = \frac{Q(X)}{\vartheta_o X} \frac{3600}{\text{h}} = 3600 \times 0.0356 C U \left(\frac{l}{Re}\right)^{1/5}$$

There is no possible analogy between friction and heat transfer unless both processes proceed from the same boundary conditions, i.e., unless the start of the thermal is coincident with the start of the hydrodynamical action. This condition was not met in our experiments because of the cold 10 cm (4 in.) long entering edge placed before the heat-dissipating plate. The unheated entrance length used by Jürges was 31 cm (12.2 in.); the length of his heated plate was 50 cm (19.7 in.); as in our tests. This discrepancy in test conditions from the theoretical

assumptions should give a lower coefficient of heat transfer relative to the calculation, but this influence appears to be negligibly small (reference 3).

Figure 6 shows the dimensionless quantity  $\frac{Q(X)}{\vartheta_0 X C U}$  against the Reynolds Number. My own experiments check very closely with Jürges' tests. The shape of the measured curve also is similar to that of the theoretical curve. The marked discrepancy of the theoretical curve, which is contrary to what was expected according to the above consideration, is probably due to the fact that the assumption  $\frac{Re}{Pe} = \epsilon = 1$  does not hold.

In my tests  $\epsilon = 1.38$ . Under these circumstances there really is a certain arbitrariness as to the presence of Re. If Pe is used instead of Re, it changes the coefficient of heat transfer in the ratio of

$$\sqrt[5]{\epsilon} = \sqrt[5]{1.38} = 1.065,$$

whereby the theoretical curve approaches the test points by 6.5 percent. Pchlhausen's theoretical curve (reference 7) is valid for the laminar range. Here

$$Q(X) = A(\sigma) \lambda_L \vartheta_0 (Re)^{1/2}$$

For our case  $\sigma = \frac{1}{\epsilon} = 0.73$ .  $A(\sigma) = 0.594$ . Our own test points lie in the turbulent zone.

Figure 7 gives the experimental results in logarithmic plotting. They may be illustrated by a straight line

The exponent  $n$  in  $\frac{Q(X)}{\vartheta_0 X C U} = \text{const} \left(\frac{1}{Re}\right)^n$  is 0.22, against Kármán's  $n=0.2$ .

The finned plates.— By comparing the recorded temperatures and heat outputs of the finned plates with the analysis, it was attempted to ascertain the extent of permissibility between the omissions made in the theory of the fins and the assumptions for the practical calculation of the heat dissipation and temperature conditions.

The assumptions 1, and 3 to 6, are complied with in our experiments and also in the majority of cases in practice. Assumption 2, that is, coefficient of heat transfer constant over the whole fin surface, does not hold.

To begin with,  $\alpha$  changes in stream direction along the plate. It is highest at the nose of the plate and drops toward the plate end. The results of the flat plate are representative of the course  $\alpha$  with the plate length. Then there is the change of  $\alpha$  over the fin side perpendicular to the flow direction.

The investigation of the velocity and temperature field in the air between the fins manifested a drop in velocity at the fin root and a rise in velocity relative to the conditions prevailing at the tip. Figures 8 and 9 give as examples for finned plate No. 1, the lines of equal temperature and velocity between the fins at  $\vartheta_0 = 39.2^\circ\text{C}$  and  $U = 25.6$  m/s. The temperature and velocity gradient in all investigated cases decreased perpendicularly to the fin surface from the fin tip toward the root.

From this it may be inferred that the coefficient of heat transfer also decreases from the fin tip toward the root. Harper and Brown estimate the decrease of  $\alpha$  from tip to root at 10 to 15 percent at the most. Bogaerts (reference 8) obtained considerably greater deviations from the recorded temperature distribution in a round fin (maximum difference about 50 percent). Besides, his maximum is not at the fin head but at about one third to one half of the fin depth from the root. To what effects this surprising result is attributable, is difficult to explain. As far as our own experiments are concerned, the fact that theory and experiment are largely in accord, makes such marked variability of  $\alpha$  improbable.

Fin temperatures.— Examples of recorded temperature curves for different finned plates and velocities are given in figures 10 to 15, that is, the temperature versus the fin depth at point  $x = 420$  mm (16.54 in.) and the temperature at the fin tip versus the plate length. The temperature of the fin side dropped as the air velocity increased. The temperature drop, i.e., the reduction in effectiveness of the fin surface increases with the thinness of the fin. For a certain velocity the temperature at the fin tip rises at first rapidly with increasing distance from the plate border, then more slowly. Here the influence of the changeability of the coefficient of heat transfer with the plate length, becomes apparent.

The comparison of theory and test data was made as follows: We established a mean value for  $\alpha$  over the whole

surface of the fin arrangement, that is, fin sides including the area between the fins. Then we defined the mean temperature of the total surface from the recorded temperature curve.

#### NOTATION

- $\bar{\theta}$ , mean temperature over the air of the whole surface ( $^{\circ}\text{C}$ ).
- $\alpha$ , mean coefficient of heat transfer for the total surface ( $\text{k cal/m}^2 \text{ h } ^{\circ}\text{C}$ ).
- $F$ , total surface ( $\text{m}^2$ ).
- $Q(X)$ , heat dissipation per meter surface per second and quantity of heat dissipation up to point X ( $\text{k cal/m s}$ ).
- $\theta_0$ , base surface temperature over the air ( $^{\circ}\text{C}$ ).
- $\alpha_0$ , coefficient of heat transfer referred to base surface ( $\text{k cal/m}^2 \text{ h } ^{\circ}\text{C}$ ).
- $F_0$ , base surface = flat-plate surface ( $\text{m}^2$ ).
- $Q_p$ , heat dissipation of test plate ( $\text{k cal/h}$ ).

Equation  $\alpha F \bar{\theta} = \alpha_0 F_0 \theta_0 = Q_p$  gives:

$$\alpha = \alpha_0 \frac{F_0}{F} \frac{\theta_0}{\bar{\theta}} = \frac{Q_p}{F \bar{\theta}}$$

With this value for  $\alpha$ , we computed the temperature in the fin conformably to the previously deduced equation for the triangular fin:

$$\frac{\bar{\theta}}{\theta_0} = \frac{J_0 \left( 2i \sqrt{\frac{\alpha}{\lambda z_0}} \sqrt{y h} \right)}{J_0 \left( 2i \sqrt{\frac{\alpha}{\lambda z_0}} h \right)}$$

Figures 16 to 21 show the computed and the recorded temperatures.

The fin-tip temperature is plotted against the mean coefficient of heat transfer stipulated as basis of the calculation. Owing to the variability of  $\alpha$  over the plate

length the figures recorded for  $x = 80$ ,  $x = 166$ ,  $x = 250$ , and  $x = 420$  mm (3.15, 6.53, 9.84, and 16.54 in. respectively) cannot agree with the theoretical figure. For that reason, we formed the average of the tip temperature over the plate length from the measurements. The comparison of the thus defined mean temperatures at the fin tip with the theoretical curve for the triangular fin is ostensibly agreeable.

The appended figures include the temperature versus fin depth for different cases compared with the analysis. The temperatures recorded at  $x = 166$  mm and  $x = 420$  mm are plotted. Here also the experimental values at  $x = 166$  mm and  $x = 420$  mm cannot exactly agree with the theoretical result because of the variability of  $\alpha$  with the plate length. The theoretical curve lies between the two measured curves. It is readily seen that here also the theoretical value as mean value over the plate length is representative of the conditions.

In all investigated fins the recorded temperatures over the fin depth evince a systematic deviation from the theoretical curve. The experimental curve has a consistently greater curvature, while the theoretical curve is more nearly a straight line. This discrepancy is greatest in the curves for finned plates 1 and 3, which had fins of identical dimensions; only the fin spacing of No 1 was 30 mm (11.8 in.), and that of No. 3, 15 mm (0.6 in.). A comparison of the fin-tip temperature for both plates, in fig. 19 manifests a close agreement.

The discrepancy between the theoretical and the experimental curve is attributable to the influence of the finite thickness at the fin tip, which was from 0.8 to 1.0 mm (0.03 to 0.04 in.). In the finned plates 1 and 3, which showed the greatest discrepancy between theory and experiment, the thickness ratio of fin tip to fin root  $z_h/z_0$  is greatest.

In one case we computed the temperature course for the exact wedge shape according to the above cited equations.

Figure 21 shows the theoretical curves for the triangular and the wedge-shaped fins. The assumption of more pronounced curvature of the temperature curve due to the finite thickness of the fin tip, is substantiated. The

theoretical curve for the wedge-shaped fin discloses an even greater curvature and a higher fin-tip temperature than the experimental curve, so that the recorded mean fin-tip temperature lies between the theoretical figures for the triangular and for the wedge-shaped fin.

The location of the theoretical curve for the wedge shape at the fin tip above the experimental is a result of the simplifying boundary condition introduced in the differential equation, namely, that  $d\theta/dy = 0$  at the fin tip. This means that the heat dissipation at the fin head is disregarded.

The exact condition should read:

$$\lambda \frac{d\theta}{dy} = \alpha \theta,$$

which, however, would complicate the equations for the wedge-shaped fin, already very unwieldy, even more.

In most practical cases the equations for the triangular fin can be employed except when  $z_h/z_0$  assumes abnormally high values. Even if the computed temperature curves of the two fin specimens manifest the discrepancies outlined above, the calculation of the heat output of the fins discloses only very small differences. For the above-cited case, finned plate No. 3:

$$U = 14.95 \text{ m/s}$$

$$\alpha = 38.8 \left[ \frac{\text{k cal}}{\text{m}^2 \text{ h } ^\circ\text{C}} \right]$$

the heat output of the finned plate is

$$\alpha_0 = 234.5 \left[ \frac{\text{k cal}}{\text{m}^2 \text{ h } ^\circ\text{C}} \right]$$

on the basis of the equations for wedge-shaped fin. With the equations for the triangular fin the approximate calculation disclosed

$$\alpha_0 = 231 \left[ \frac{\text{k cal}}{\text{m}^2 \text{ h } ^\circ\text{C}} \right]$$

The difference is 1.5 percent. In this case the quantity  $u$  in figure 2, which gives the heat performance curves of the triangular and rectangular fins, equals 1.22. For increasing  $u$ , that is, for increasing  $\alpha$  with the same fin profile, the difference between the approximate and the more exact calculation, is slightly greater.

Heat performance of finned plates.— The heat output of a flat plate fitted with fins comprises the heat given off by the fins and that of the plate lying between the fins.

For an assumed equal coefficient of heat transfer, the heat dissipation of the finned plate is:

$$Q_p = 2n X \left( \frac{Q}{\vartheta_0} \right) \vartheta_0 + (b - 2n z_0) X \vartheta_0 \alpha = \alpha_0 F_0 \vartheta_0.$$

Here  $n$  = number of fins,

$X$  = length in flow direction,

$\frac{Q}{\vartheta_0}$  = heat output per meter of fin side  $k$  cal/m h °C,

$b$  = width of finned plate,

$z_0$  = semithickness of fins at root.

This gives:

$$\alpha_0 = \frac{2n X}{F_0} \left( \frac{Q}{\vartheta_0} \right) + \frac{(b - 2n z_0) X}{F_0} \alpha.$$

and inserting the value  $Q/\vartheta_0$  for the triangular fin, we have:

$$\alpha_0 = \frac{2n X}{F_0} \sqrt{\alpha \lambda z_0} \frac{-i J_1 \left( 2i \sqrt{\frac{\alpha}{\lambda z_0}} h \right)}{J_0 \left( 2i \sqrt{\frac{\alpha}{\lambda z_0}} h \right)} + \frac{(b - 2n z_0) X}{F_0} \alpha$$

This formula was used for plotting  $\alpha_0$  against  $\alpha$  in figure 22. The experimental  $\alpha_0$  are in close agreement with the calculation. Therefore the calculation of the heat output of finned plates by means of the above formula in conjunction with a mean value for  $\alpha$  is permissible.

Thus the preliminary calculation of a fin assembly exposed to air at a stated speed is possible when the mean  $\alpha$  for the particular arrangement is known. I have attempted - on the basis of the test data - to develop an empirical formula for  $\alpha$  applicable with any fin arrangement and velocity.

To this end I resorted to Taylor and Rehbeck's report on fin elements (reference 9), and compared their data with our own. Their experiments were made on copper plates in a closed-throat tunnel at velocities of from 20 to 70 m/s (65.62 to 229.7 ft./sec.). (See table III.) The plates were 6 inches square; the fins were 1 inch deep and 0.20 inch thick. The fin spacing for the nine plates ranged between 1/2 inch to 1/12 inch. The results are shown in figure 23, where  $\alpha_0$  is plotted against air velocity  $U$ .

As Taylor and Rehbeck failed to determine the mean coefficient of heat transfer  $\alpha$  for their experiments, and likewise omitted the temperature distribution in the fins, we defined  $\alpha$  by means of equation:

$$\alpha_0 = \frac{2n X}{F_0} \left( \frac{Q}{\vartheta_0} \right) + \frac{(b - 2n z_0) X}{F_0} \alpha$$

With the  $Q/\vartheta_0$  value for the rectangular fin, the equation reads:

$$\alpha_0 = \frac{2n X}{F_0} \sqrt{\alpha \lambda z_0} \tanh \sqrt{\frac{\alpha}{\lambda z_0}} h + \frac{(b - 2n z_0) X}{F_0} \alpha$$

conforming to which, the curves  $\alpha_0 = f(\alpha)$  were computed for different plates. (See fig. 24.)

From figures 23 and 24,  $\alpha_0 = f(U)$  and  $\alpha_0 = f(\alpha)$  were determined  $\alpha$  for each plate with respect to  $U$ .

Figure 25 illustrates in logarithmic plotting the nondimensional quantity:

$$\frac{Q(x)}{\vartheta X C U} = \frac{\alpha}{3600 C U}$$

versus the Reynolds Number for Taylor and Rehbeck's experiments, while our corresponding test data (see also table

II) are given in figure 26. Equation

$$\frac{Q(x)}{\rho X C U} = k f \left( \frac{1}{Re} \right)$$

corresponds to the relation cited previously for the flat plate.

Every fin arrangement is accompanied by such an equation, whereby quantity  $k$  for each arrangement has a definite value dependent upon the hydrodynamically influential dimensions.

In general, we can therefore put:

$$\frac{Q(x)}{\rho X C U} = k_1 f \left( \frac{1}{Re} \right) f_1 (X; a'; h)$$

where  $a'$  = mean inside spacing between each fin,

$h$  = fin depth,

$X$  = length in flow direction.

Figures 25 and 26 reveal that within the explored range  $f \left( \frac{1}{Re} \right)$  is suitably expressed by a power function.

We write:

$$\frac{Q(x)}{\rho X C U} = k_1 \left( \frac{1}{Re} \right)^{n(X; a'; h)} f_1 (X; a'; h).$$

Here  $n$  is again a function of  $X$ ,  $a'$ , and  $h$ .

Now we could surmise that  $n$  and  $f_1$  were functions of  $\frac{a'}{h}$  and  $a'h$ ;  $\frac{a'}{h}$  is the aspect ratio,  $a'h$  the section of the air passage formed by two fins. The most elementary nondimensional combination of the quantities  $\frac{a'}{h}$ ,  $a'h$ , and  $X$  is:

$$\frac{X}{\frac{a'}{h} \sqrt{a'h}} = \frac{X}{\beta}$$

The transition from finned to flat plate may be effected in simple fashion, either with  $h = 0$  or with  $a'$

infinitely great. In both cases:

$$\beta = \infty; \quad \frac{X}{\beta} = 0.$$

The  $\frac{Q(x)}{\beta X C U}$  values are plotted against  $\frac{X}{\beta}$  for  $Re = 4 \times 10^5$  in figure 27. Our own test points are quite in accord with those of Taylor and Rehbock, excepting the points  $\frac{X}{\beta} = 18$  and  $\frac{X}{\beta} = 34$  of the finned plates at 1/2 and 1/3 inch spacing.

The obtained interdependence of coefficient of heat transfer  $\alpha$  and  $\beta$  implies the following: If, under otherwise identical conditions, the fin depth is made  $m$  times as great, the inside fin spacing  $a$  must be made  $\sqrt[3]{m}$  as great in order to assure the same coefficient of heat transfer.

Accordingly, the general equation for the coefficient of heat transfer on finned and flat plates reads:

$$\frac{Q(x)}{\beta X C U} = k_1 \left(\frac{1}{Re}\right)^n \left(\frac{X}{\beta}\right)^{f_1\left(\frac{X}{\beta}\right)}$$

Figure 28 shows  $n = f\left(\frac{X}{\beta}\right)$ ;  $n$  drops at first from 0.22 for the flat plate as  $X/\beta$  increases, then less rapidly and assumes the then constant value 0.12 at about  $\frac{X}{\beta} = 140$ .

This regularity is, of course, valid only for a stated range of Reynolds Number. For very high velocities, i.e., high Reynolds Numbers, the curves  $Q(x)/\beta X C U = f(UX/v)$  in figures 25 and 26 approach asymptotically the curve for the flat plate. In reality the curves are curved lines rather than straight lines, but may be closely approximated by straight lines for the explored range.

$$\text{Figure 29 gives } \frac{Q(x)}{\beta X C U} \left(\frac{UX}{v}\right)^n = f\left(\frac{X}{\beta}\right).$$

Each dot represents a finned plate. Our test data and those of Taylor and Rehbock are in close agreement. As their finned plates and air velocities were altogether different from ours, it is possible to apply the data on the basis of the results to other arrangements also; that is, in the neighborhood of the examined Reynolds Numbers and with fin spacing wide enough to avoid laminar flow between the fins.

With the above limitations the coefficient of heat transfer  $\alpha$  relative to the air velocity can be computed for any fin arrangement with the aid of figures 28 and 29. It is possible to so define the fin dimensions and distances for a base surface of stated size that the heat performance  $\alpha_0$  of the base surface gives a maximum for a stated air velocity or for a limited part of it. The procedure for solving this important practical problem is as follows:

The conventional form of the fin is wedge-shaped because it is easy to manufacture and utilizes the material quite satisfactorily. The amount of material for a fin rises as the 3d power of the heat output, consequently the fin depth will be kept as small as consistent with structural reasons, but in place of that the number of fins may be increased. Starting from the fin thickness, the height of the fin is determined on the basis of an appraisal of  $\alpha$ , so as to approach the optimum dimensions as closely as possible. Then the fin spacing may be ascertained at which the heat output of the base surface is maximum. The realization of appropriate fin dimensions assumes here particular significance, because in the interest of a very high coefficient of heat transfer it is important not to unnecessarily reduce the flow section available between the fins.

Grateful acknowledgment of indebtedness is here made to Professor Dr. Th. v. Kármán for his invaluable aid in this report, and to the Society for the Support of Science in Germany for the means of the experimental equipment.

Translation by J. Vanier,  
National Advisory Committee  
for Aeronautics,

## REFERENCES

1. Harper, D. R., 3d, and Brown, W. B.: Mathematical Equations for Heat Conduction in the Fins of Air-Cooled Engines. T.R. No. 158, N.A.C.A., 1923.
2. Schmidt, E.: Die Wärmeübertragung durch Rippen. Z.V.D.I., June 26, and July 10, 1926, pp. 885 and 947.
3. Elias, Franz: The Transference of Heat from a Hot Plate to an Air Stream. T.M. No. 614, N.A.C.A., 1931.
4. Hütte, vol. I, 26th ed., p. 506.
5. Jürges, W.: Der Wärmeübergang an einer ebenen Wand. Beih. z. Gesundh.-Ing. München: Oldenbourg, 1924.
6. Von Kármán, Th.: Über laminare und turbulente Reibung. Abhdlg. d. Aerodyn. Inst. d. T.H. Aachen, no. 1, p. 1.  
  
Latzko, H.: Der Wärmeübergang an einen turbulenten Flüssigkeits- oder Gasstrom. Abhdlg. d. Aerodyn. Inst. d. T.H. Aachen, no. 1, p. 36.
7. Pohlhausen, E.: Der Wärmeaustausch zwischen festen Körpern und Flüssigkeiten mit kleiner Reibung und kleiner Wärmeleitung. Z. angew. Math. Mech., 1921, p. 120.
8. Bogaerts, M.: Het Temperatuursverloop in Koelribben en de Berekening dezer Ribben. Delft: W. D. Meinema.
9. Taylor, C. Fayette, and Rehbock, A.: Rate of Heat Transfer from Finned Metal Surfaces. T.N. No. 331, N.A.C.A., 1930.

TABLE I. Dimensions of Test Plates

	Length x mm	Width b mm	a mm	a' mm	h mm	z <sub>0</sub> mm	z <sub>h</sub> mm	$\beta = \frac{a'}{h} \sqrt{a'h}$ cm	$\frac{X}{\beta}$	s mm	Material
Flat plate	499	209	-	-	-	-	-	$\infty$	0	10	Ultralumin
Finned plate No. 1	500	210	30	28.2	45.0	1.4	0.4	2.23	22.4	10	"
" " No. 2	500	210	30	24.5	45.3	5.0	0.5	1.81	27.6	10	Silumin
" " No. 3	500	210	15	13.0	45.2	1.5	0.5	0.698	71.7	10	"
" " No. 4	500	210	15	9.5	45.0	5.0	0.5	0.437	114.5	10	"
" " No. 5	500	210	15	11.3	45.1	3.0	0.7	0.567	88.0	10	"
" " No. 6	500	210	15	12.1	22.3	2.5	0.4	0.893	56.0	10	"

mm x 0.03937 = in.

cm x 0.3937 = in.

Table II. Experimental values for investigated plates.  
Flat plate  $n = 0.22$

$U$ m/sec	$Re$	$Pe$	$\alpha_0$ kcal m <sup>2</sup> h °C	$\alpha$ kcal m <sup>2</sup> h °C	$\frac{\alpha}{3600 C \bar{U}}$	$\alpha \left(\frac{UX}{\nu}\right)^n$ $\frac{\alpha}{3600 C \bar{U}}$	Average
9,5	2,78 · 10 <sup>5</sup>	2,01 · 10 <sup>5</sup>	34,8		0,00382	0,0603	
12,55	3,72 · 10 <sup>5</sup>	2,7 · 10 <sup>5</sup>	42,7		0,00352	0,0592	
15,05	4,4 · 10 <sup>5</sup>	3,2 · 10 <sup>5</sup>	50,7		0,00350	0,0608	
19,15	5,63 · 10 <sup>5</sup>	4,08 · 10 <sup>5</sup>	60,0		0,00325	0,0597	
19,3	5,61 · 10 <sup>5</sup>	4,08 · 10 <sup>5</sup>	60,9		0,00328	0,0602	
24,7	7,1 · 10 <sup>5</sup>	5,16 · 10 <sup>5</sup>	73,5		0,00312	0,0603	
28,6	8,18 · 10 <sup>5</sup>	5,96 · 10 <sup>5</sup>	81,9		0,00302	0,0601	
33,9	9,5 · 10 <sup>5</sup>	6,95 · 10 <sup>5</sup>	94,2		0,00293	0,0606	
41,7	11,45 · 10 <sup>5</sup>	8,33 · 10 <sup>5</sup>	110,5		0,00285	0,0612	0,0603
<b>Finned plate I <math>n = 0,195.</math></b>							
9,1	2,6 · 10 <sup>5</sup>	1,87 · 10 <sup>5</sup>	105,0	29,5	0,00341	0,0389	
14,8	4,33 · 10 <sup>5</sup>	3,16 · 10 <sup>5</sup>	149,5	44,1	0,00305	0,0384	
19,8	5,75 · 10 <sup>5</sup>	4,19 · 10 <sup>5</sup>	182,0	55,6	0,00291	0,0386	
25,6	7,46 · 10 <sup>5</sup>	5,42 · 10 <sup>5</sup>	216,0	68,5	0,00275	0,0384	
34,8	9,8 · 10 <sup>5</sup>	7,07 · 10 <sup>5</sup>	259,5	85,2	0,00260	0,0383	0,0385
<b>Finned plate II <math>n = 0,187.</math></b>							
8,9	2,58 · 10 <sup>5</sup>	1,87 · 10 <sup>5</sup>	100,3	28,2	0,00331	0,0340	
14,7	4,27 · 10 <sup>5</sup>	3,09 · 10 <sup>5</sup>	148,0	42,1	0,00299	0,0338	
19,9	5,75 · 10 <sup>5</sup>	4,17 · 10 <sup>5</sup>	188,5	54,3	0,00286	0,0340	
19,9	5,62 · 10 <sup>5</sup>	4,08 · 10 <sup>5</sup>	186,0	53,6	0,00286	0,0339	
25,7	7,32 · 10 <sup>5</sup>	5,3 · 10 <sup>5</sup>	229,0	67,0	0,00274	0,0342	
34,9	9,7 · 10 <sup>5</sup>	6,97 · 10 <sup>5</sup>	286,0	84,8	0,00260	0,0342	
42,0	11,6 · 10 <sup>5</sup>	8,43 · 10 <sup>5</sup>	328,5	98,8	0,00251	0,0341	0,0340
<b>Finned plate III <math>n = 0,14.</math></b>							
9,1	2,6 · 10 <sup>5</sup>	1,88 · 10 <sup>5</sup>	152,0	24,4	0,00286	0,0164	
14,95	4,38 · 10 <sup>5</sup>	3,18 · 10 <sup>5</sup>	230,5	38,8	0,00268	0,0165	
20,0	5,87 · 10 <sup>5</sup>	4,26 · 10 <sup>5</sup>	284,0	49,5	0,00256	0,0164	
25,6	7,30 · 10 <sup>5</sup>	5,25 · 10 <sup>5</sup>	341,0	61,4	0,00254	0,0167	
30,1	8,90 · 10 <sup>5</sup>	6,40 · 10 <sup>5</sup>	387,0	71,7	0,00245	0,0167	
35,0	10,15 · 10 <sup>5</sup>	7,38 · 10 <sup>5</sup>	428,0	81,0	0,00239	0,0166	
41,0	12,0 · 10 <sup>5</sup>	8,7 · 10 <sup>5</sup>	466,0	90,0	0,00228	0,0162	0,0165
<b>Finned plate IV <math>n = 0,122.</math></b>							
9,1	2,63 · 10 <sup>5</sup>	1,91 · 10 <sup>5</sup>	135,0	22,2	0,00255	0,0117	
15,0	4,26 · 10 <sup>5</sup>	3,08 · 10 <sup>5</sup>	208,0	34,6	0,00245	0,0116	
18,8	5,61 · 10 <sup>5</sup>	4,05 · 10 <sup>5</sup>	259,0	43,3	0,00237	0,0119	
20,0	5,78 · 10 <sup>5</sup>	4,18 · 10 <sup>5</sup>	273,0	45,7	0,00238	0,0120	
25,6	7,37 · 10 <sup>5</sup>	5,34 · 10 <sup>5</sup>	334,0	56,4	0,00230	0,0119	
30,1	8,62 · 10 <sup>5</sup>	6,25 · 10 <sup>5</sup>	379,0	64,8	0,00226	0,0119	
34,7	9,7 · 10 <sup>5</sup>	7,07 · 10 <sup>5</sup>	425,0	73,5	0,00224	0,0120	
41,2	11,23 · 10 <sup>5</sup>	8,2 · 10 <sup>5</sup>	472,0	82,7	0,00218	0,0119	0,0119
<b>Finned plate V <math>n = 0,13.</math></b>							
9,1	2,66 · 10 <sup>5</sup>	1,91 · 10 <sup>5</sup>	152,0	23,9	0,00276	0,0140	
15,1	4,42 · 10 <sup>5</sup>	3,19 · 10 <sup>5</sup>	238,0	38,1	0,00263	0,0143	
15,1	4,44 · 10 <sup>5</sup>	3,2 · 10 <sup>5</sup>	235,5	37,7	0,00261	0,0142	
20,0	5,85 · 10 <sup>5</sup>	4,22 · 10 <sup>5</sup>	300,0	49,1	0,00256	0,0144	
20,0	5,85 · 10 <sup>5</sup>	4,22 · 10 <sup>5</sup>	299,0	49,0	0,00256	0,0144	
25,5	7,37 · 10 <sup>5</sup>	5,34 · 10 <sup>5</sup>	358,0	59,9	0,00247	0,0143	
25,6	7,52 · 10 <sup>5</sup>	5,45 · 10 <sup>5</sup>	363,0	60,7	0,00245	0,0142	
30,2	8,67 · 10 <sup>5</sup>	6,28 · 10 <sup>5</sup>	401,0	68,0	0,00238	0,0141	
34,8	9,9 · 10 <sup>5</sup>	7,17 · 10 <sup>5</sup>	445,0	76,8	0,00235	0,0142	
41,2	11,63 · 10 <sup>5</sup>	8,43 · 10 <sup>5</sup>	507,0	89,0	0,00229	0,0141	0,0142
<b>Finned plate VI <math>n = 0,157.</math></b>							
9,3	2,64 · 10 <sup>5</sup>	1,91 · 10 <sup>5</sup>	96,0	26,4	0,00300	0,0212	
14,8	4,28 · 10 <sup>5</sup>	3,1 · 10 <sup>5</sup>	143,0	39,6	0,00280	0,0213	
20,55	5,82 · 10 <sup>5</sup>	4,22 · 10 <sup>5</sup>	184,0	51,2	0,00265	0,0212	
25,7	7,26 · 10 <sup>5</sup>	5,26 · 10 <sup>5</sup>	218,0	61,2	0,00253	0,0210	
30,2	8,53 · 10 <sup>5</sup>	6,18 · 10 <sup>5</sup>	249,5	70,4	0,00246	0,0209	
35,7	9,86 · 10 <sup>5</sup>	7,16 · 10 <sup>5</sup>	280,0	79,5	0,00239	0,0209	
42,1	11,58 · 10 <sup>5</sup>	8,42 · 10 <sup>5</sup>	324,0	92,7	0,00236	0,0211	0,0211

TABLE III. Taylor and Rehbock Experiments

Fin spacing a inches	1/2	1/3	1/4	1/6	1/7	1/8	1/9	1/10	1/12
$\frac{K}{\beta}$	18.0	34.0	54.5	106.7	140	177	218	266	376
n	0.2	0.18	0.16	0.123	0.12	0.12	0.12	0.12	0.12
$\alpha \left( \frac{U X}{v} \right)^n$ mean value	0.0367	0.0283	0.0206	0.0120	0.0121	0.0114	0.0113	0.0106	0.0091

3600 CU

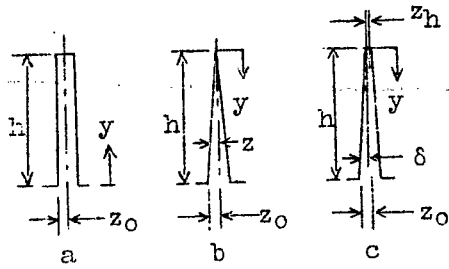


Figure 1.

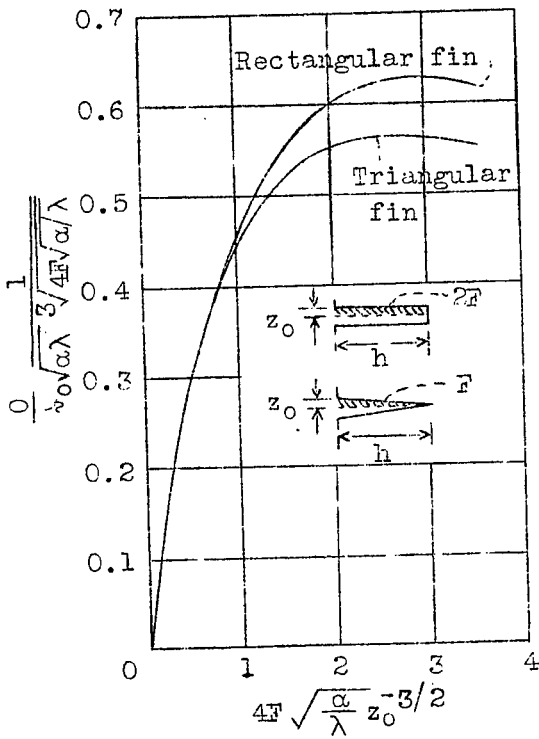
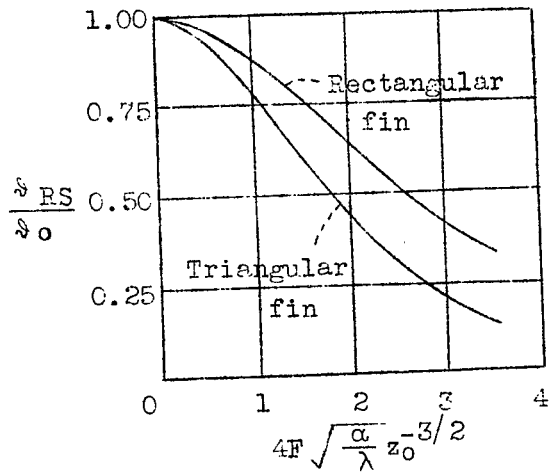


Figure 2.- Heat output of a straight fin.

Figure 3.- Temperature at fin tip.



- a, 900 mm  
35.43 in.
- b, 500 mm  
19.68 in.
- c, 340 mm  
13.39 in.
- d, 210 mm  
8.27 in.
- e, 100 mm  
3.94 in.
- f, 90 mm  
3.54 in.
- g, 50 mm  
1.97 in.

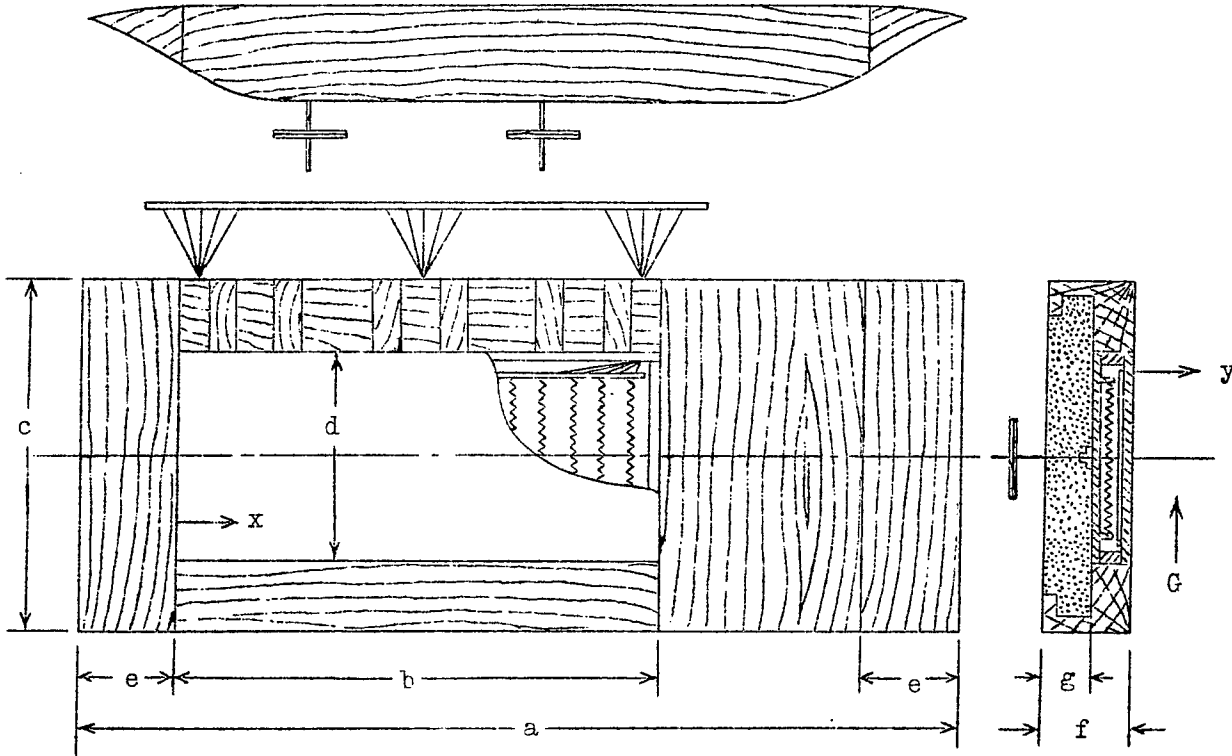


Figure 4.- Experimental frame.

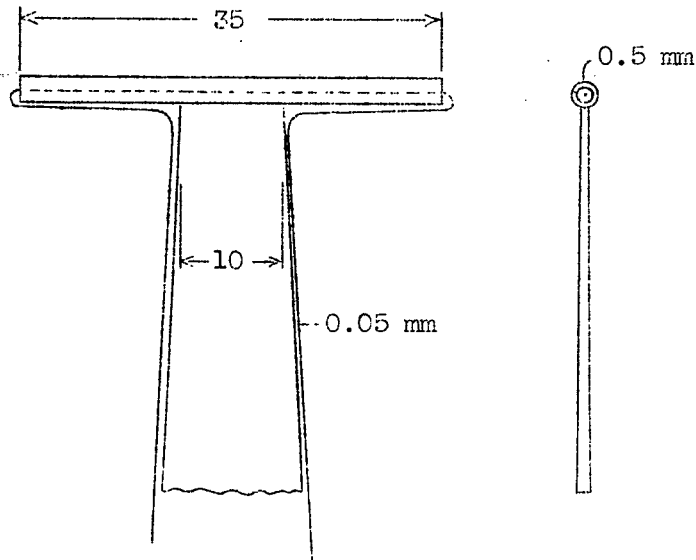


Figure 5.-Diagram of boundary layer thermocouple.

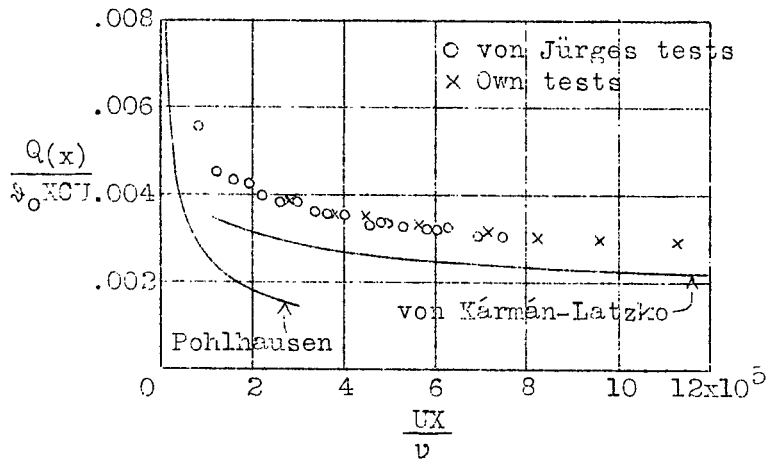


Figure 6.-Coefficients of heat transfer for the flat plate.

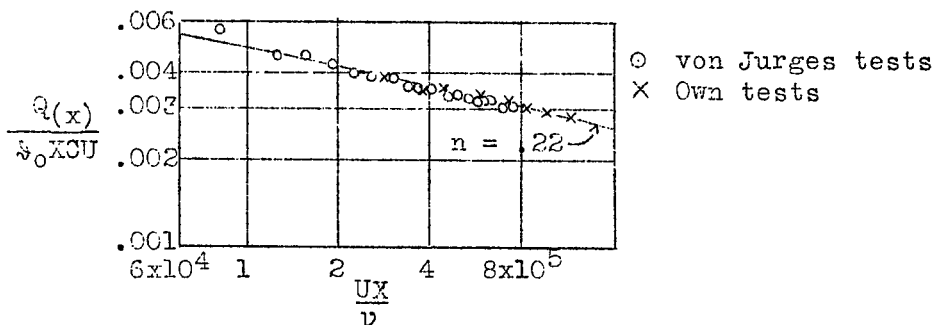


Figure 7.-Coefficients of heat transfer for the flat plate.

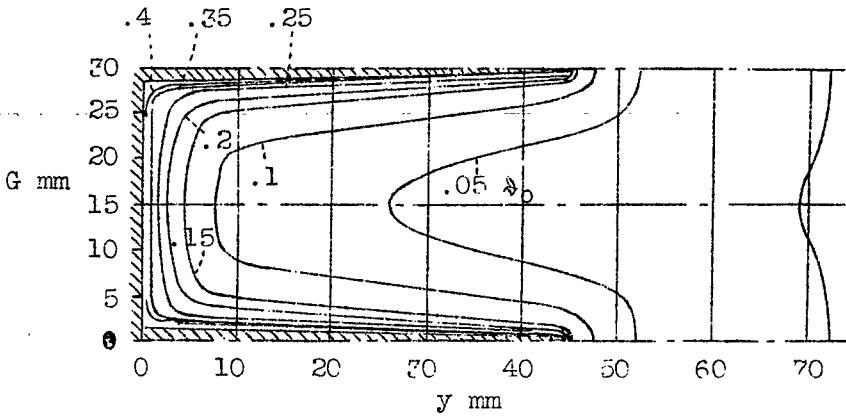


Figure 8.-  
Temperature  
distribution  
in the air  
between the fins;  
finned plate I.  
 $\theta_0 = 79.2^\circ\text{C}$ ;  
 $U = 25.6 \text{ m/sec}$ .

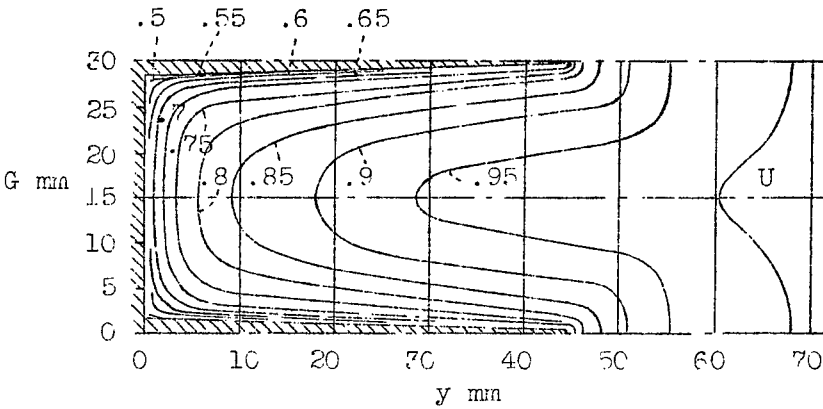


Figure 9.-  
Velocity  
distribution  
between the fins;  
finned plate I.  
 $U = 25.6 \text{ m/sec}$ .

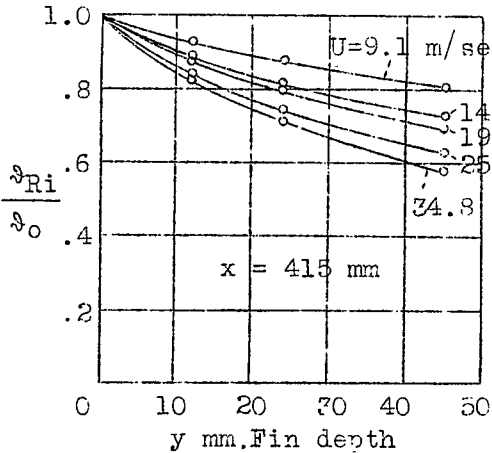


Figure 10.- Fin temperature,  
recorded at  
 $x = 415 \text{ mm}$ .  
Finned plate I.

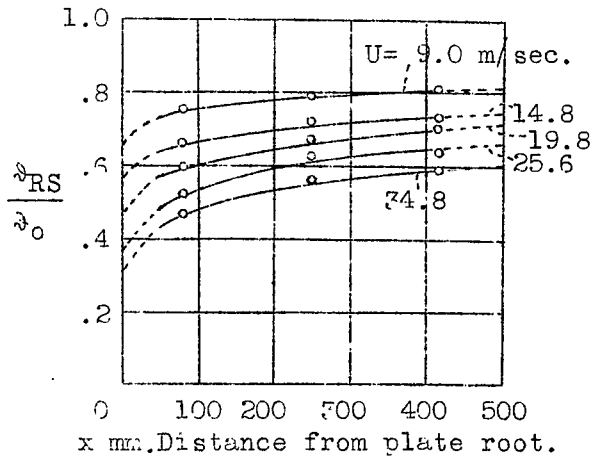


Figure 11.- Temperature at fin tip;  
finned plate I.

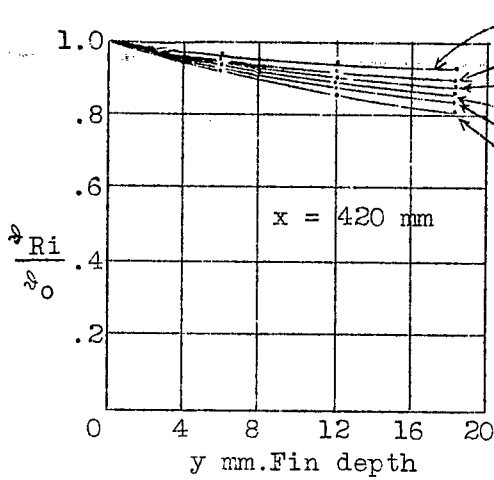


Figure 12.-Fin temperature recorded at  $x = 420$  mm, finned plate II.

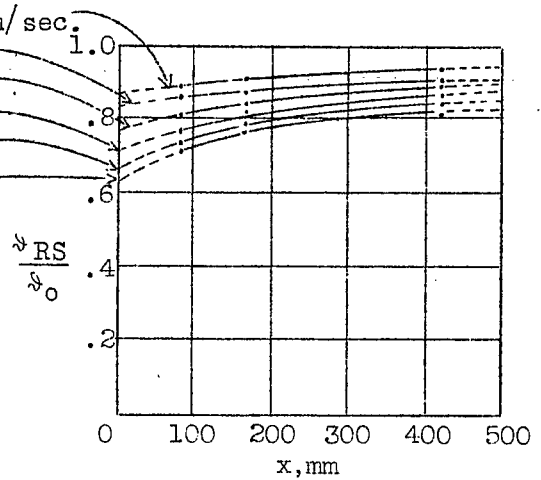


Figure 13.-Fin tip temperature; finned plate II.

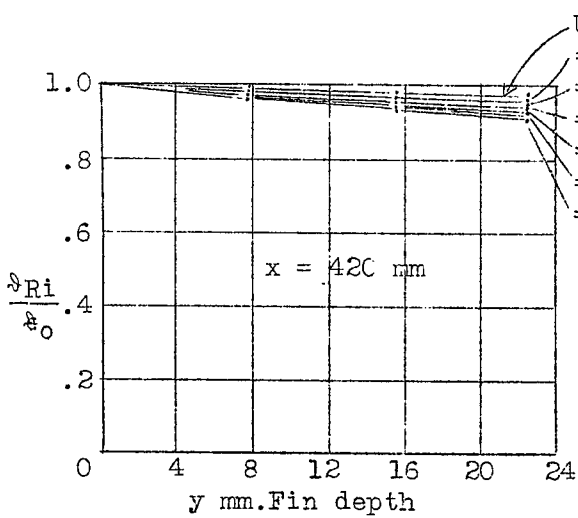


Figure 14.-Fin temperature recorded at  $x = 420$  mm, finned plate VI.

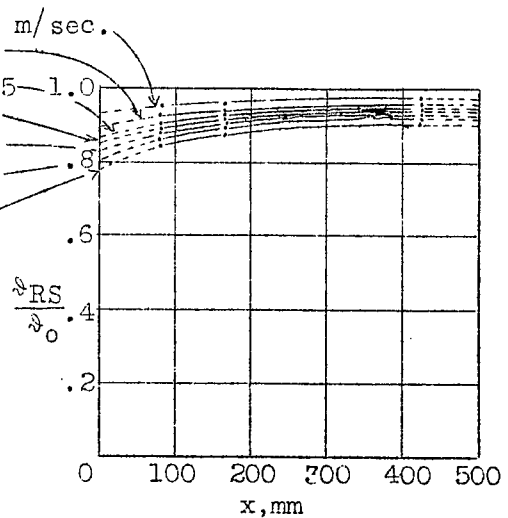


Figure 15.-Fin tip temperature; finned plate VI.

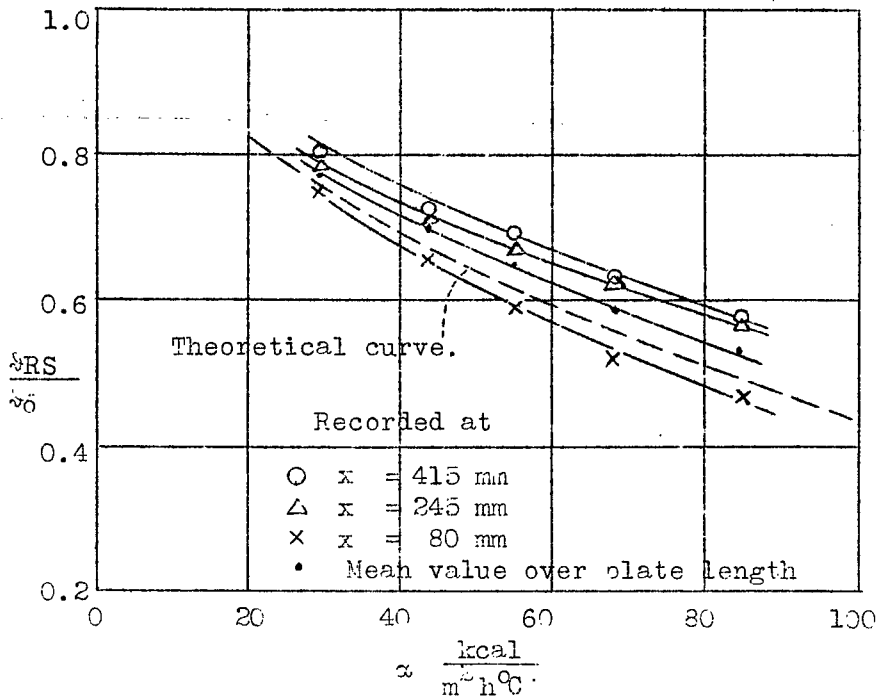


Figure 16.- Fined plate I, fin tip temperature, analysis compared with experiment.

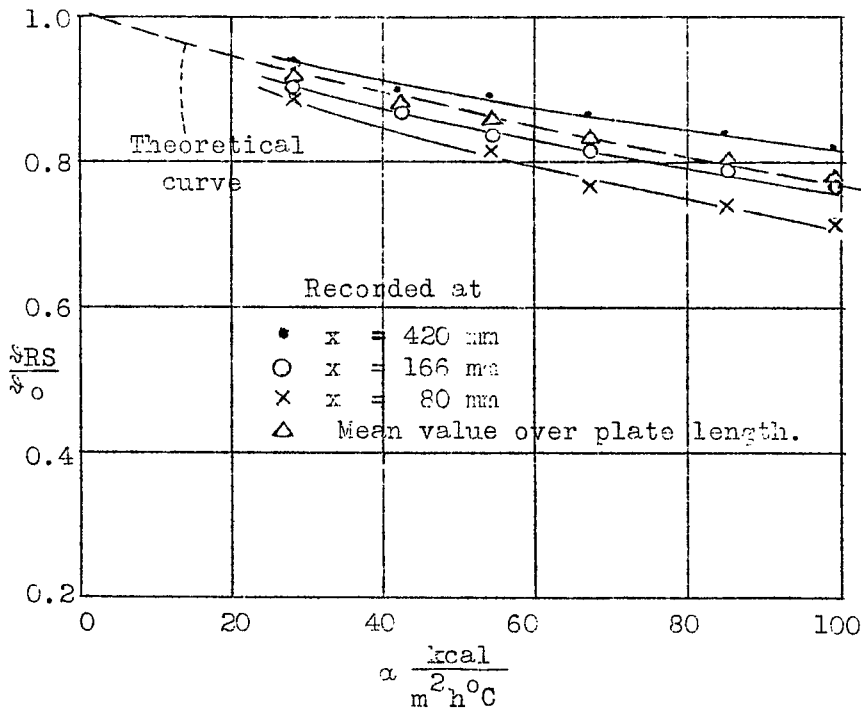


Figure 17.- Fined plate II, fin tip temperature, analysis compared with test.

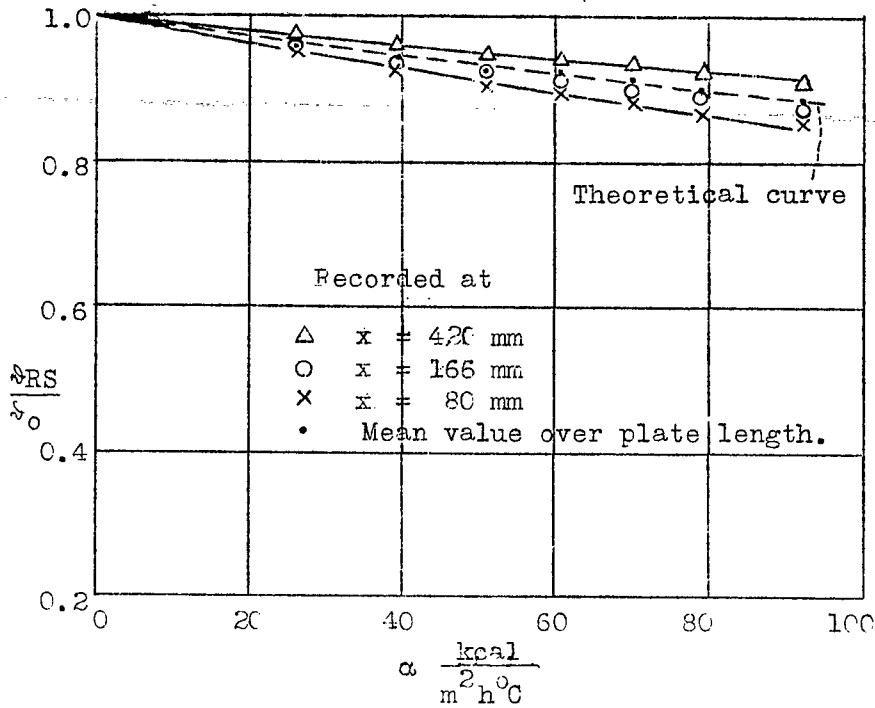


Figure 18.- Finned plate VI, fin tip temperature, theory versus experiment.

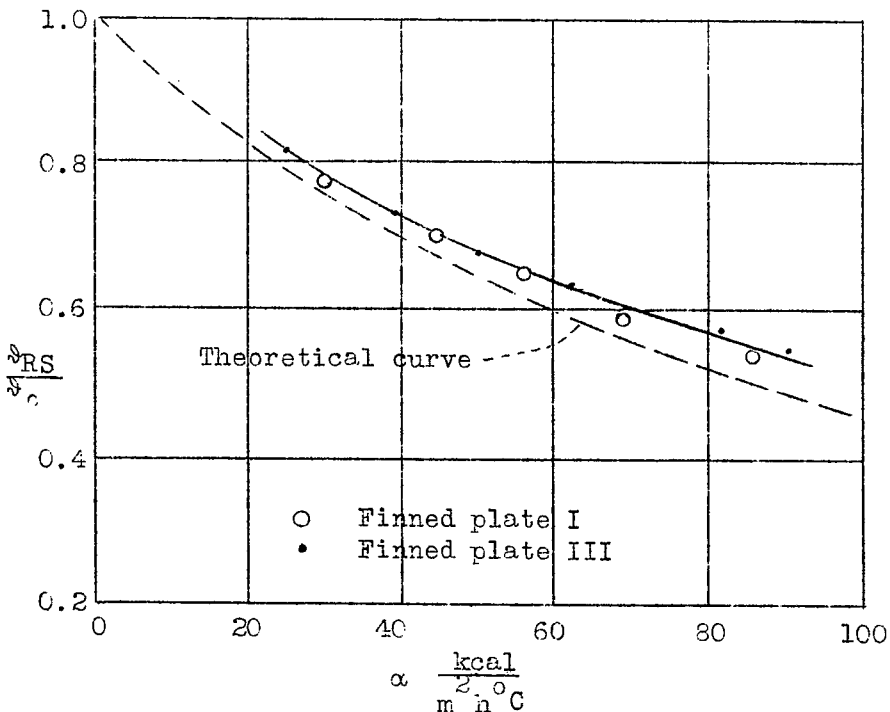
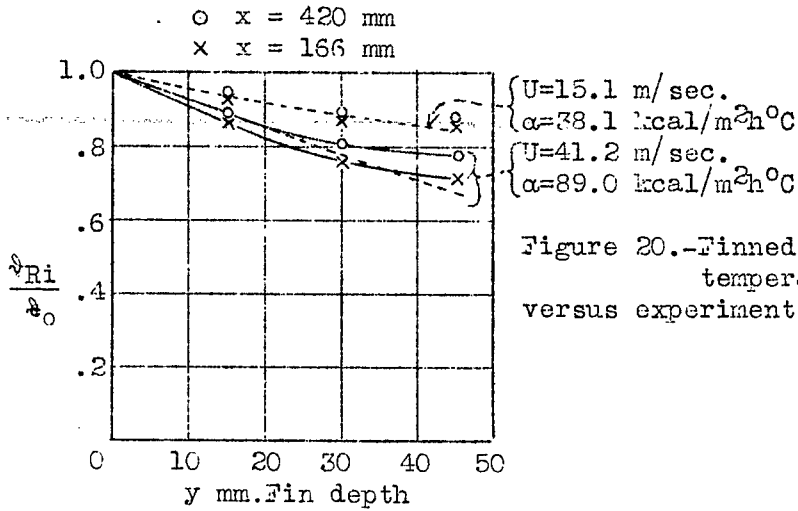
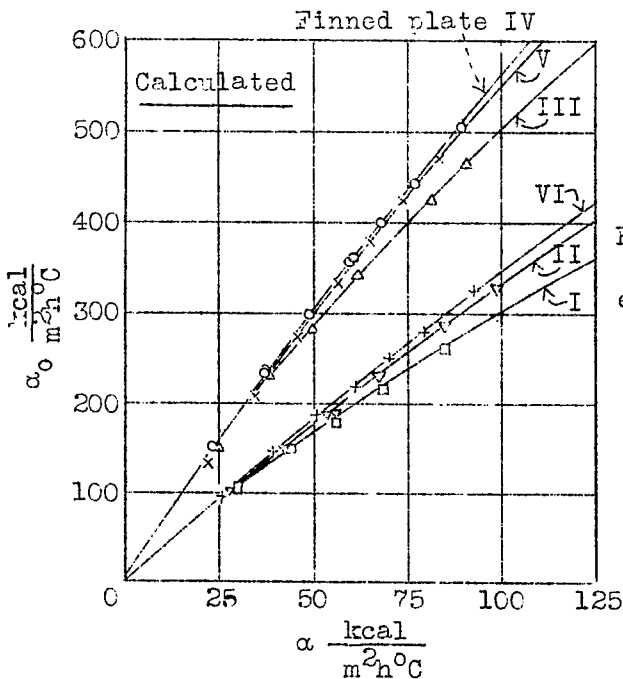
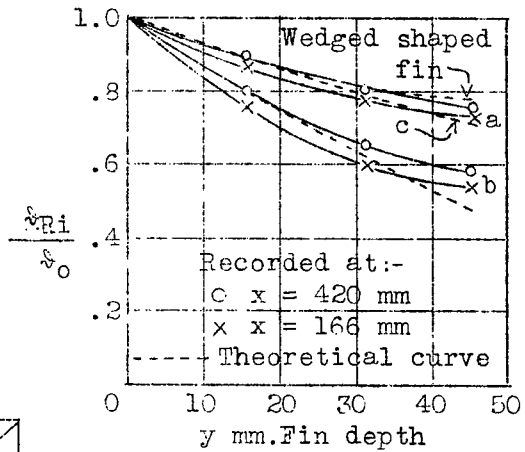


Figure 19.- Fin tip temperature, finned plate I compared with finned plate III.



- a,  $U=14.95$  m/sec,  $\alpha=38.8$  kcal/m<sup>2</sup>h<sup>°</sup>C
- b,  $U=41.0$  m/sec,  $\alpha=90.0$  kcal/m<sup>2</sup>h<sup>°</sup>C
- c, Triangular fin.

Figure 21.-Finned plate III; fin temperature; theory versus experiment.



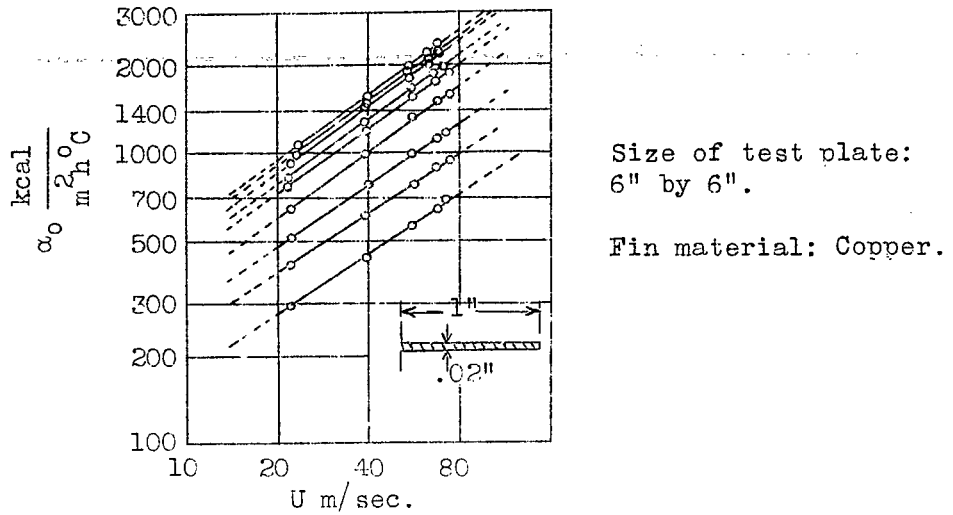


Figure 23.-- Heat output of finned plates-  
Taylor and Rehbock: test data.

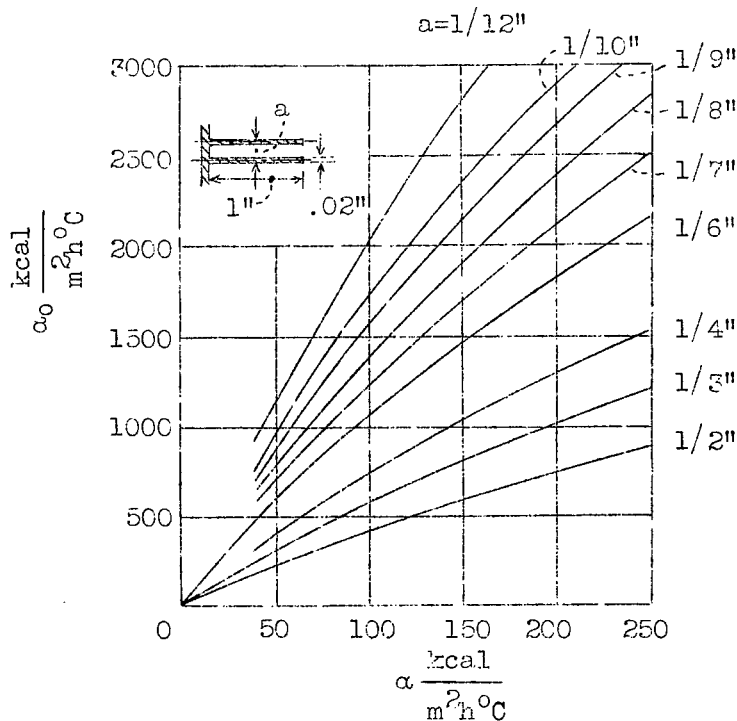


Figure 24.-- Theoretical heat output of finned plates-  
Taylor and Rehbock data.

Fin spacing					
No. 1	1/2"	n = 0.20	No. 5	1/7"	n = 0.12
2	1/7	.18	6	1/8	.12
3	1/4	.16	7	1/9	.12
4	1/6	.123	8	1/10	.12
			9	1/12	.12

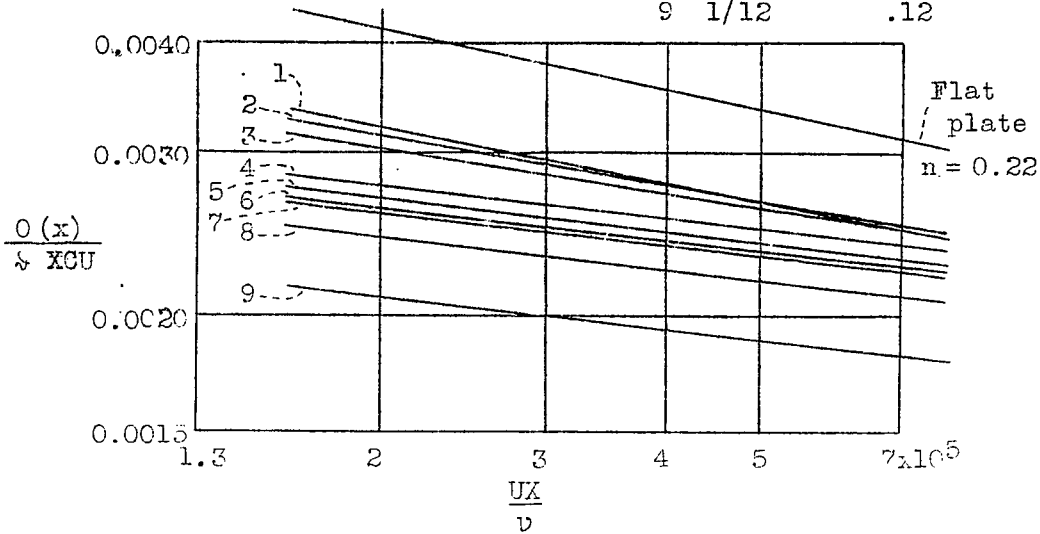


Figure 25.- Coefficient of heat transfer for Taylor-Rehbock specimens.

Finned plate	n	Finned plate	n
△ I	0.195	▽ IV	0.122
○ II	.187	× V	.130
• III	.140	+ VI	.157

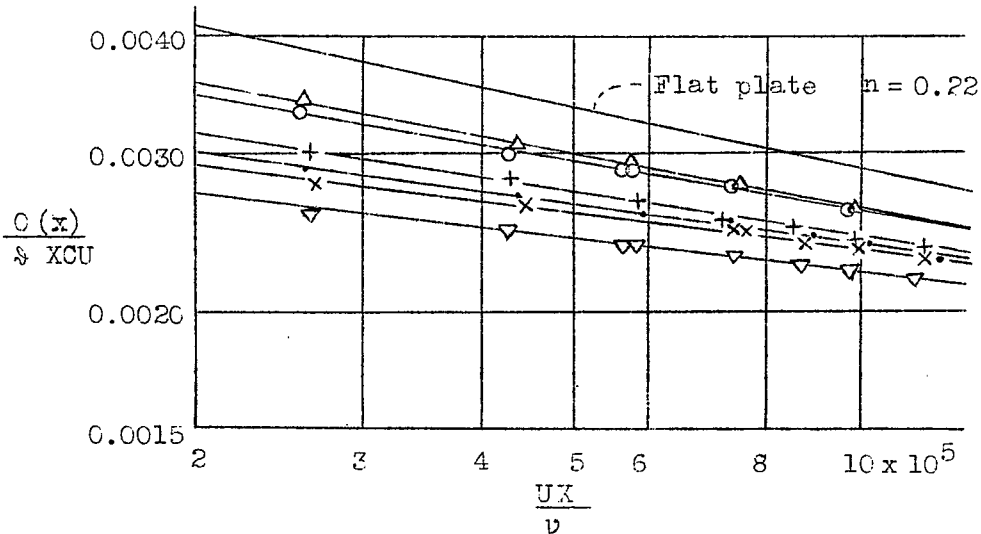


Figure 26.- Coefficient of heat transfer for explored profiles for finned plates I to VI.

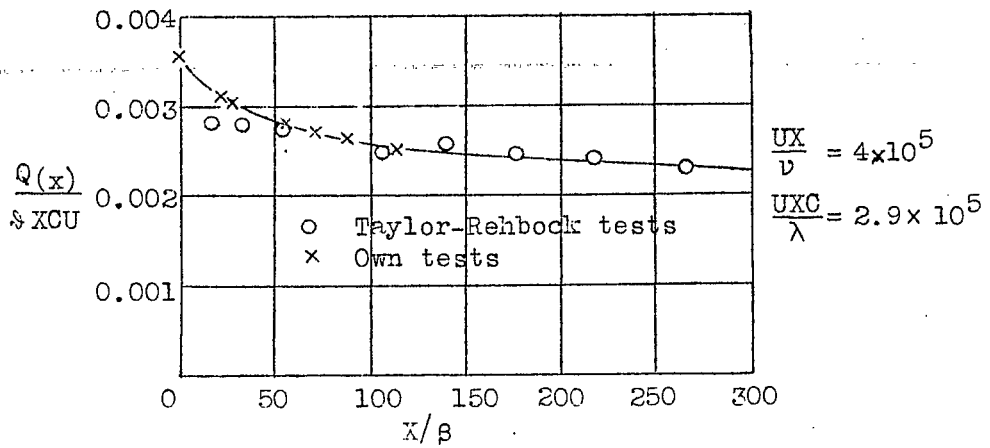


Figure 27.- Comparison of experimental values at  $R = 4 \times 10^5$  with Taylor-Rehbock records.

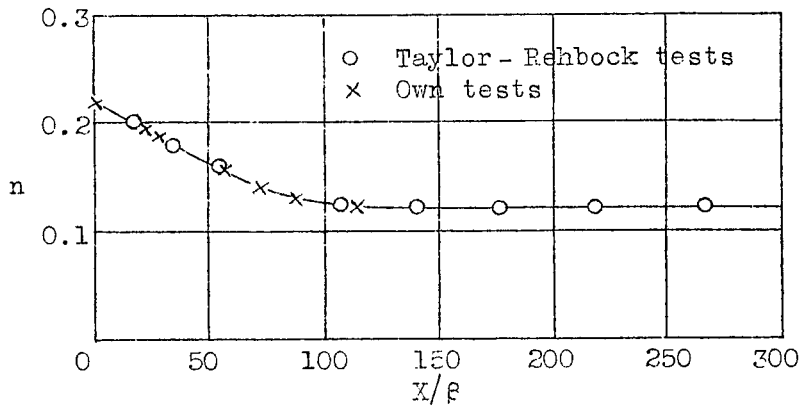


Figure 28

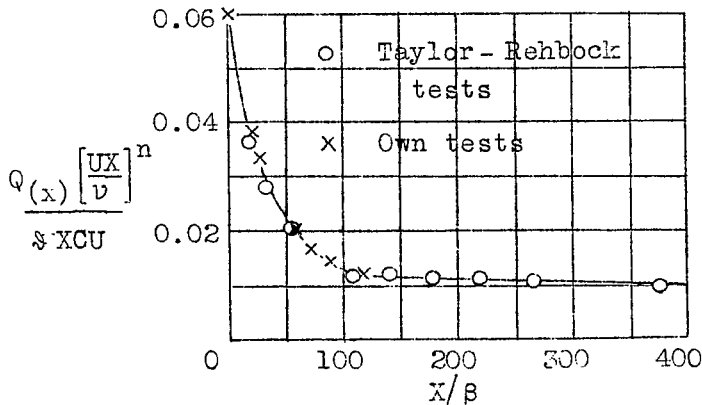


Figure 29.- Coefficient of heat transfer for flat and finned plates.

NASA Technical Library



3 1176 01441 1509